

Studies on Amorphous Alloy Dispersed Aluminium Matrix Composite Prepared by High Pressure Torsion

S. Hembrom¹, B. N. Roy¹, N. Khobragade² & D. Roy²

¹ Department of Metallurgical Engineering, BIT, Sindri, Dhanbad-828123, India

² Department of Materials and Metallurgical Engineering, NIFFT, Ranchi-834003, India

Correspondence: D. Roy, Department of Materials and Metallurgical Engineering, NIFFT, Ranchi-834003, India. Tel: 91-651-229-1125. E-mail: droy2k6@gmail.com

Received: October 1, 2015 Accepted: October 26, 2015 Online Published: December 29, 2015

doi:10.5539/jmsr.v5n1p89

URL: <http://dx.doi.org/10.5539/jmsr.v5n1p89>

Abstract

Aluminium-based composite reinforced with Cu base amorphous alloy dispersed composite was prepared by means of high pressure torsion between a powder mix of aluminium and amorphous Cu base alloy. The X-ray diffraction pattern of powdered and consolidated composites shows the aluminium phase while the thermal stability of the amorphous alloy was studied with the aid of differential scanning calorimetry (DSC). The microstructural feature of the composite through scanning electron microscope reveals the well-distributed reinforcements in the host aluminium matrix. The hardness measurement on the as prepared composites shows significant increase in hardness with increase in reinforced amorphous alloy. Wear property of the synthesized composites were measured by using ball on plate wear tester which shows increase in wear resistance with increase in reinforced amorphous alloys.

Keywords: metal matrix composite, amorphous alloy, mechanical properties, electron microscopy, high pressure torsion

1. Introduction:

Aluminum (Al)-based metal matrix composites (MMCs) make up a distinct category of advanced engineering materials that provide unique advantages over conventional Al alloys. With the development of new forming methods and the use of low cost particulate material, the use of these composites is increasing in a wide variety of industries. Particulate reinforced composites consist of a uniform distribution of strengthening particles within a matrix. In general, these materials exhibit good wear and erosion resistance, as well as higher stiffness, hardness and strength at a lower density when compared to the unreinforced matrix material (Wielage, Zschunke, Henker, & Steinhäuser, 1996). Recently metal matrix composites (MMCs) are increasingly used for critical structural and wear resistant applications because of their excellent strength to weight ratio (Clyne & Withers, 1995) and interesting physical properties. In the last few decades, MMCs, and in particular aluminium (Al)-based MMCs, are receiving increasing application as aerospace and automotive components because of high specific strength and stiffness (Harrington, 1994). Normally MMCs are reinforced with continuous fibers, discontinuous particles or whiskers. However, particle-reinforced MMCs possess some distinct advantages over fiber-reinforced composites in terms of low cost and isotropic mechanical property. In general, reinforcement particulates are prepared independently prior to composite fabrication and are incorporated into the metal matrix at a later stage. The composites so developed are called *ex situ* MMCs. Al composite have the advantage of low cost over most other metal matrix composites. In addition to the above they offer excellent abrasion resistance, high temperature operation, non-flammability, minimum attack by fuels & solvents, and their ability to be formed and treated on conventional equipments. The performance of MMCs can further be improved by refining the grain structure and the size of reinforcement particles to nano-metric range (Harrington, 1994) and (Yamasaki et al., 2003). Recent investigations find that incorporation of nano-particles into the aluminum matrix could enhance the hardness, the yield and ultimate tensile strength considerably, while the ductility retained (Mazahery, Abdizadeh, & Baharvandi, 2009).

It has been investigated earlier that amorphous materials can be synthesized by mechanical alloying of the elemental powder constituents of different Al-based binary and higher order alloys, e.g. Al-Ti (Lee, Sim, Heo, Cho, & Kwon, 2000), Al-Fe (Kleiner, Bertocco, Khalid, & Belfort, 2005), and Al-Ti-Si (Lv et al., 2001). However, in none of these alloys, amorphous microstructures could be obtained in bulk quantity at relatively slow or normal

solidification rate. Cu–Zr based bulk metallic glasses (BMGs) attracted high attention because of their relatively low costs (Pauly, Das, Mattern, Kim, & Eckert, 2009; Louzguine-Luzgin et al., 2012; Zhang, Chen, Zheng, & Chen, 2013). Aluminum has been regarded as useful element to improve the plasticity of the Cu-Zr-based BMGs (Wu et al., 2011). The addition of minor Al quantities (up to 10 at.%) to the Cu–Zr glassy alloys may improve their thermal stability, mechanical properties and glass forming ability (GFA) (Cheung & Shek, 2007; Lee, Jo, & Lee, 2013). Research is therefore in progress to find out other possible Al-based alloy compositions, which can either retain a completely amorphous structure or an amorphous-nanocrystalline aggregate. Such developments are expected to pave the way for fabricating bulk amorphous materials in future. In the present work aluminium based composites synthesized by reinforcing Cu base amorphous alloy by high pressure torsion and the microstructure and mechanical properties have been investigated.

2. Experimental

2.1 Processing of Amorphous $\text{Cu}_{50}\text{Zr}_{45}\text{Al}_5$ Powder

Amorphous $\text{Cu}_{50}\text{Zr}_{45}\text{Al}_5$ powder was prepared from commercially available micron sized powders of $\text{Cu}_{50}\text{Zr}_{45}\text{Al}_5$ by dry mechanical milling (cryo milling, -196°C) performed in a planetary ball mill. During milling, the weight ratio of the ball to the powder was maintained at 10:1. The balls and vials are made of tungsten carbide. The rotating speed of the vial was maintained at 300 rpm. Milling was stopped after 4 hr and powder samples were collected.

2.2 Processing of Composites

Aluminium powder of 99% purity with an average particle size $\sim 10\mu\text{m}$ (Loba Chemie Pvt. Ltd., Mumbai) and amorphous $\text{Cu}_{50}\text{Zr}_{45}\text{Al}_5$ powder prepared by dry mechanical milling were mixed thoroughly. The different weight percentages of amorphous $\text{Cu}_{50}\text{Zr}_{45}\text{Al}_5$ powder were mixed with aluminium for composite as shown in the Table: 1

Table 1. Different wt% of amorphous alloys in different samples

Sl. No.	Weight % of Aluminium	Weight % of amorphous $\text{Cu}_{50}\text{Zr}_{45}\text{Al}_5$ powder
1.	100	0
2.	90	10
3.	80	20
4.	70	30
5.	60	40

The powder **mixture**, so prepared, was subsequently compacted in cylindrical (10mm dia.) graphite dies under an applied pressure of 50 MPa in a hot press (Fritschkg Postfech-500428, Germany) at 200°C . The pressing load on the specimen was applied for 15 min after the desired temperature was attained. The sample was then allowed to cool to room temperature and the cylindrical samples were stripped from the graphite die for characterization. Hot pressing was followed by high pressure torsion (HPT) under an applied pressure of 1GPa was used for full densification and Al-matrix grain refinement.

2.3 Characterization

XRD studies on the $\text{Cu}_{50}\text{Zr}_{45}\text{Al}_5$ powder prior to and after ball milling were recorded by using $\text{Cu-K}\alpha$ radiation. Hot pressed composite samples were also characterized by XRD technique using a Panalytical X'Pert Pro diffractometer with $\text{Cu K}\alpha$ radiation. Prior to the analyses, the XRD patterns were corrected for the effects of the $\text{K}\alpha_2$ radiation. The particle size of the ball milled $\text{Cu}_{50}\text{Zr}_{45}\text{Al}_5$ powders were evaluated from the XRD patterns. Microscopic studies to examine the morphology and distribution of particles in the synthesized composites were done by a JEOL 6480 LV scanning electron microscope (SEM). The thermal stability of the amorphous powder, were studied under argon gas atmosphere with the aid of a differential scanning calorimeter (DSC, Mettler, TA400). The flow rate of argon gas was maintained at 80cc/min throughout the experiment. The powder were heated from room temperature to 800°C at a predetermined heating rate of $10^\circ\text{C}/\text{min}$ and then cooled to room temperature at a cooling rate of $10^\circ\text{C}/\text{min}$. The density of synthesized aluminium based composites was calculated by using Archimedes principle.

Average values of hardness on different phases of the composite samples were measured with the help of a standard Vickers hardness tester (Type 3212, Zwick, Ulm Germany) using a load of 25 gf applied for 15s. Sliding wear

resistance of the samples was evaluated using a ball on plate wear testing instrument having a hardened ball (SAE 52100) indenter of 6mm diameter. DUCOM TR-208-M1 ball on plate wear tester was used for evaluating the wear resistance of Al-matrix dispersed with amorphous reinforcement samples. The arrangement of the machine is such that it ensures a precise measurement of the tangential frictional force. This test method involves a ball shaped upper specimen that slides against a rotating disk as a lower specimen under a prescribed set of conditions. The load is applied vertically downward with a motor driven carriage that uses the force/load sensor for feedback to maintain a constant load. The experimental process was carried out at 10 N loads for 15 minutes at 15 rpm at an average humidity of 50-55% and at an average temperature of 25°C with steel ball. Surface damage caused by wear testing was subsequently analyzed using a scanning electron microscopy to get an idea about the wear mechanism.

3. Results and Discussion

XRD pattern reveals the phases present and the sequence of their evolution in course of mechanical alloying of the $\text{Cu}_{50}\text{Zr}_{45}\text{Al}_5$ elemental powder blend shown in Figure 1. The diffraction pattern shows the peaks of the constituent elements present in the initial mixture either disappear due to alloying, or undergo broadening and reduction in their intensity with increase in the milling time. XRD pattern reveals that the $\text{Cu}_{50}\text{Zr}_{45}\text{Al}_5$ powders prior to milling consist of peaks of Al, Cu and Zr. The similar characteristic peaks of respective elements have been reported (Azimi, Shokuhfar, & Zolriasatein, 2014). After 4 h of milling, the powders appear to constitute amorphous solid solution. The XRD diffraction pattern of milled powder shows the amorphization of $\text{Cu}_{50}\text{Zr}_{45}\text{Al}_5$ powder. Guoqiang Xie et al. (2010) studied the similar composite and reported the amorphization of milled powder.

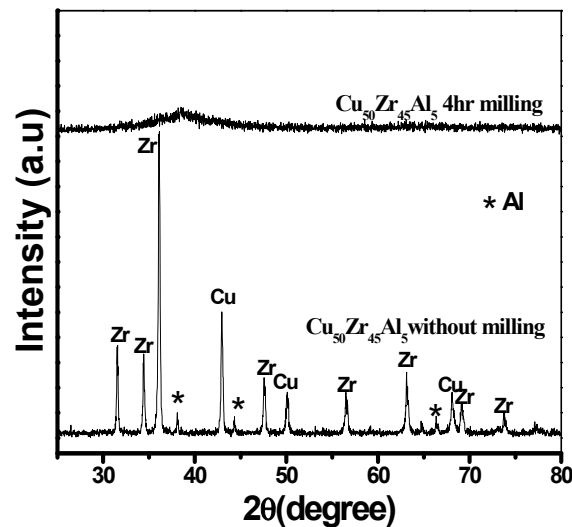


Figure 1. XRD pattern of milled and without milled $\text{Cu}_{50}\text{Zr}_{45}\text{Al}_5$ powders

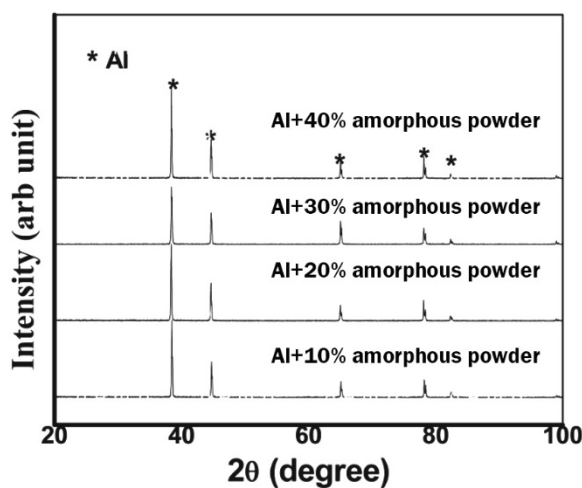


Figure 2. XRD pattern of Al+ different wt% of amorphous powder

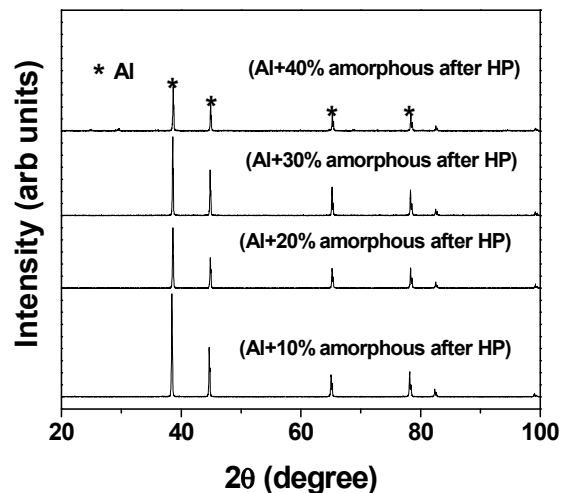


Figure 3. XRD pattern of the sample prepared by hot pressing

Figure 2 and Figure 3 show the XRD patterns of the sample in powdered form and consolidated form prepared by hot pressing respectively. Both XRD pattern revealing the presence of sharp peaks representing the phases of aluminium. The results of XRD analysis of the samples in powdered and consolidated form representing the same structure. Sharifi and Karimzadeh (2011) reported the similar diffraction peaks of aluminium in the synthesized composites.

Figure 4 shows the DSC plot obtained during heating and cooling of green compact from room temperature to 800°C and from 800°C to room temperature at a heating/cooling rate of 10°C/min under argon gas atmosphere. It is seen that, the peak obtained at 475°C, representing the amorphous- crystalline transformations. Kukuła-Kurzyniec et al. (2014) reported that the crystallization begins in the ribbon at the temperature of 437°C which is higher for the amorphous aluminium based composites. He, Bian, and Chen (2000) determined the DSC curve of bulk metallic glass $Zr_{52.5}Ni_{14.6}Al_{10}Cu_{17.9}Ti_5$ by which the T_g and T_x are reported as 631K and 710K respectively.

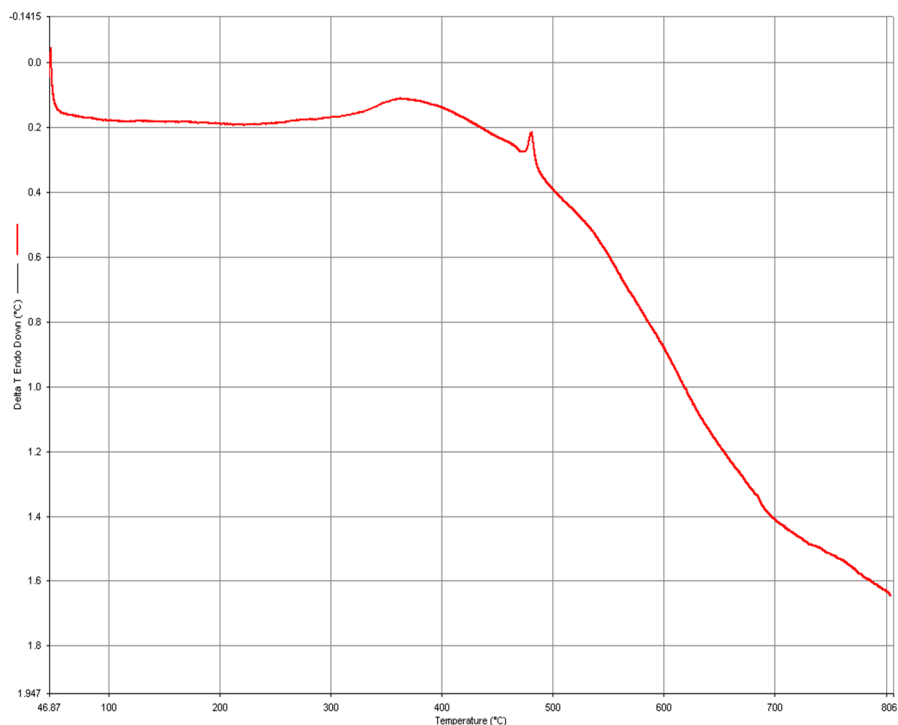


Figure 4. DSC curve for the $Cu_{50}Zr_{45}Al_5$ mechanically alloyed powders subjected to heating and cooling

SEM micrographs of the pure aluminium and composites with different weight% of amorphous alloy prepared by hot pressing at 400°C are illustrated in Figure 5(a), Figure (b), Figure (c), Figure (d), Figure (e). The microstructural feature of the composite reveals the well-distributed reinforcements (bright contrast) in the host aluminium matrix. Inference drawn from the XRD results (Figure 3) investigation suggests the absence of any constituent phase except aluminium in bright areas. Roy, Ghosh, Basumallick, and Basu (2007) reported the SEM micrographs of 10 vol% and 30 vol% reinforced Ti-aluminide content in aluminium matrix prepared by hot pressing at 700°C.

The hardness of the composites has been measured by Vickers hardness tester while densities were calculated by using Archimedes principle. Figure 6 shows the variation of density and hardness with the wt% of reinforcement of the composite samples prepared by hot pressing. On examination of the plots, it is obvious that the samples with 40% of amorphous alloy have demonstrated the highest density, which also coincides with the highest hardness. The lowest density is observed in the samples, containing 0 wt% of amorphous alloy (pure Al) due to absence of reinforcement. It has been found that the hardness of the samples increases remarkably with the increase in reinforcement content. Roy, Basu, and Mallick (2005) reveals the similar results which shows increase in hardness with increase in reinforced content in Ti-aluminide reinforced Al-based insitu metal matrix composites.

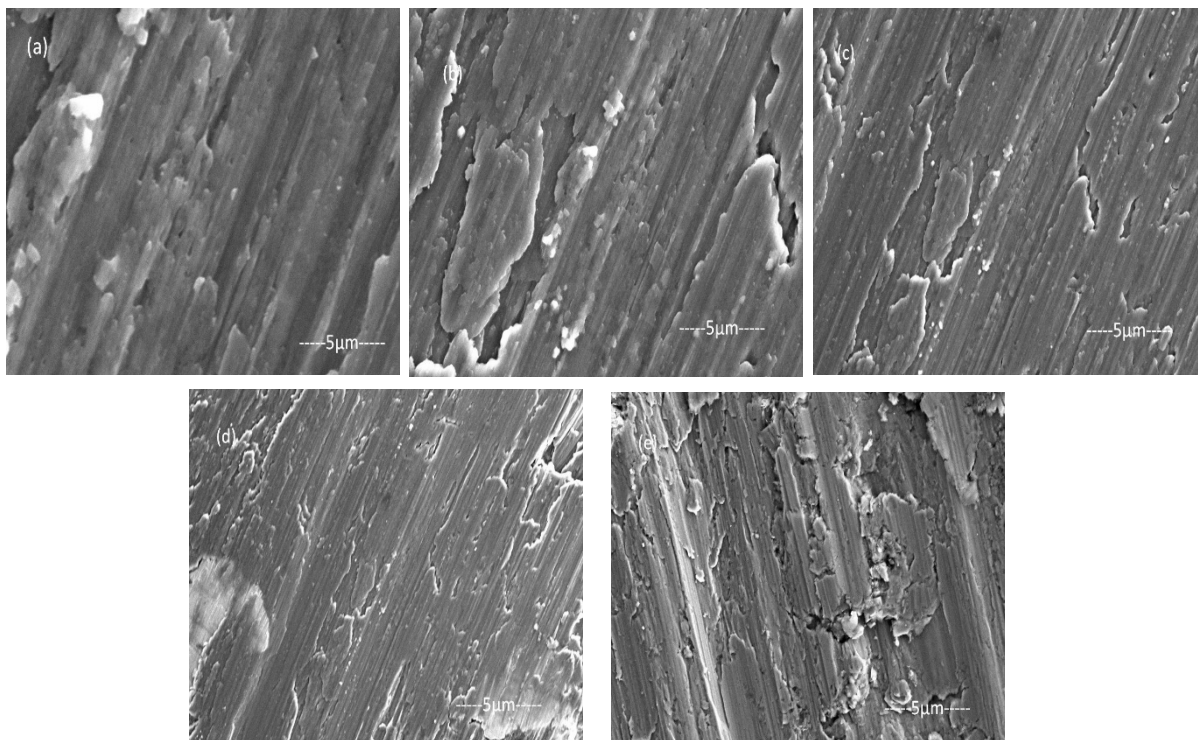


Figure 5. SEM micrographs of pure Al and composites prepared by hot pressing (a) pure Al, (b) 10% , (c) 20%, (d) 30%, (e) 40% amorphous alloy

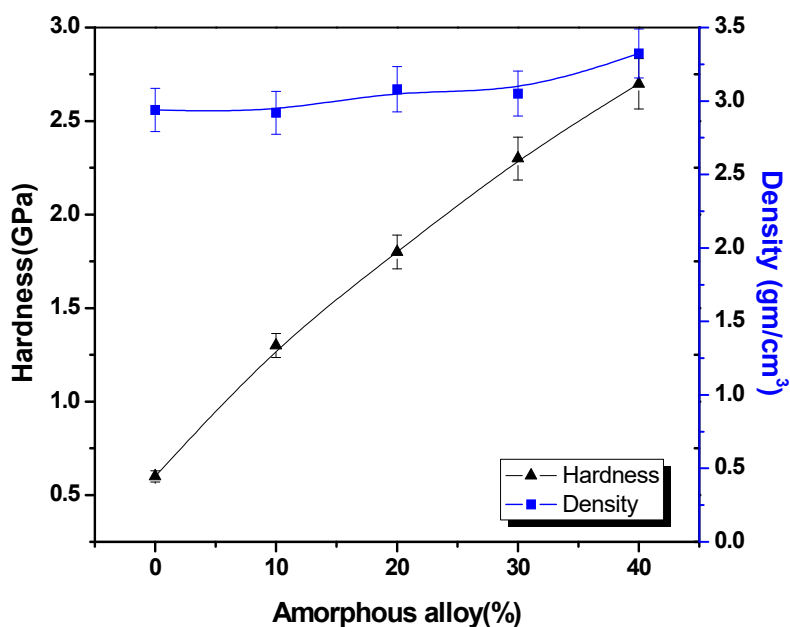


Figure 6. Density and hardness variation with respect to wt% of reinforcement of the composite samples prepared by hot pressing at 400°C

Wear properties of the designed composites were measured by using ball on plate wear test at an applied load of 10 N at 15 rpm sliding speed on a 6 mm diameter track for 15 minutes. Figure 7 shows the plot for wear depth Vs time for synthesized composites. As the microhardness results shows that hardness of the samples increases with increase in reinforced content. The similar trend was observed in wear test, 40wt % reinforced Al-matrix composite exhibit the high hardness and wear resistance. Roy, Basu, Mallick, Kumar, & Ghosh (2006) represents the similar results in Fe-aluminide reinforced Al matrix composites.

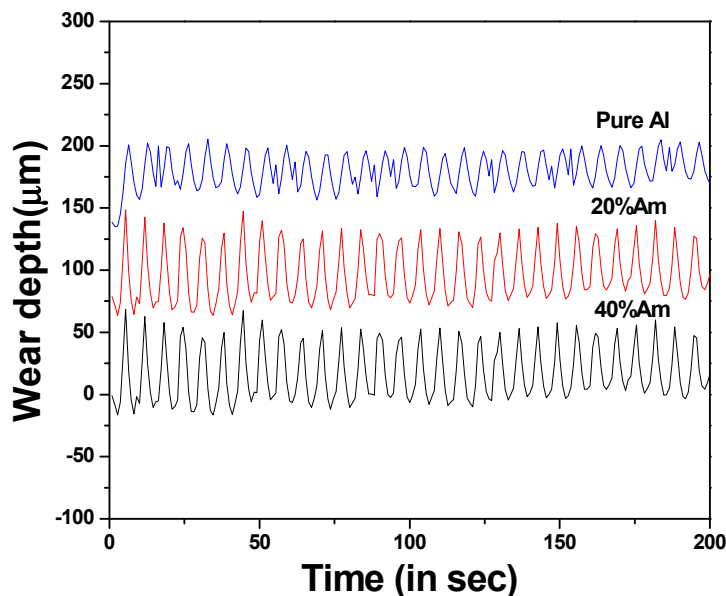


Figure 7. Plot of wear depth Vs time (in sec) for amorphous $\text{Cu}_{50}\text{Zr}_{45}\text{Al}_5$ powder content in Al-matrix

The topographical features of the worn surfaces are investigated using scanning electron microscopy in an attempt to study the wear mechanism. Figure 8 presents the overall topography of pure Al and Al-based composite reinforced with 20 and 40 wt% ex situ $\text{Cu}_{50}\text{Zr}_{45}\text{Al}_5$ powder formed, hot pressed at 400°C . For 20 wt% reinforced Al matrix, extensive plastic deformation was observed to cause more wear. The improvement in hardness due to harder amorphous $\text{Cu}_{50}\text{Zr}_{45}\text{Al}_5$ reinforcements causes increase in wear resistance of 40 wt% reinforced composite. For 40 wt% reinforcement, a transition in wear mechanism from predominantly abrasion and deformation to predominant abrasion and tribochemical wear takes place. The similar wear behavior of Al based composites were shown (Roy, Basu, & Mallick, 2005) in which Ti-aluminide is used as reinforcement in Al-matrix composite.

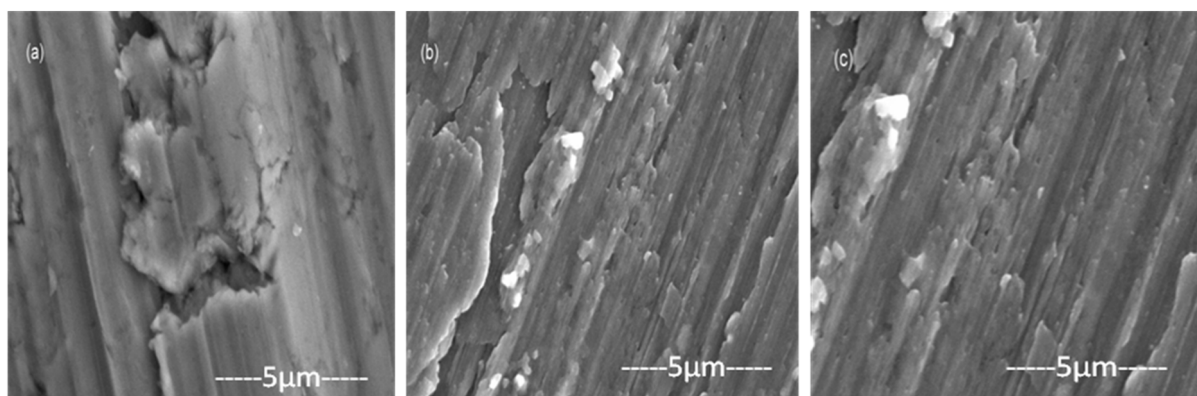


Figure 8. SEM micrograph of wear track of (a)20wt% amorphous alloy, (b)40 wt% amorphous alloy and (c) Pure Al alloy

4. Conclusion

Aluminium matrix composites reinforced with well dispersed amorphous powder prepared by hot pressing followed by high pressure torsion method. XRD pattern of both powdered and consolidated composites shows the phases of aluminium with same structure. DSC reveals that peak obtained at 475°C represents the amorphous to crystalline transformation. Microstructural architecture of amorphous alloy remains same before and after hot pressing followed by high pressure torsion. Microhardness of aluminium matrix composite reinforced with

amorphous alloy shows increase in hardness with increase in reinforcement content and similarly increase in wear resistance upto 40vol% reinforcement in synthesized composites.

References

- Azimi, A., Shokuhfar, A., & Zolriasatein, A. (2014). Nanostructured Al–Zn–Mg–Cu–Zr alloy prepared by mechanical alloying followed by hot pressing. *Materials Science and Engineering: A*, 595, 124-130.
- Cheung, T. L., & Shek, C. H. (2007). Thermal and mechanical properties of Cu–Zr–Al bulk metallic glasses. *Journal of alloys and compounds*, 434, 71-74.
- Clyne, T. W., & Withers, P. J. (1995). *An introduction to metal matrix composites*. Cambridge University Press.
- Harrington, Jr. W. C. (1994). Metal matrix composite application. In S. Ochiai (Ed.), *Mechanical properties of metallic composites* (pp. 759-73). New York: Marcel-Dekker.
- He, G., Bian, Z., & Chen, G. L. (2000). Structure evolution of bulk metallic glass Zr₅₂. 5N₁₄. 6Al₁₀Cu₁₇. 9Ti₅ during annealing. *JOURNAL OF MATERIALS SCIENCE & TECHNOLOGY*, 16(4), 357-361.
- Kleiner, S., Bertocco, F., Khalid, F. A., & Beffort, O. (2005). Reactively Synthesized Nanostructured PM Aluminium Composite–Microstructure Stability and Elevated Temperature Hardness Response. *Advanced Engineering Materials*, 7(5), 380-383.
- Kukuła-Kurzyniec, A., Dutkiewicz, J., Góral, A., Coddet, C., Dembinski, L., & Perrière, L. (2014). Aluminium based composites strengthened with metallic amorphous phase or ceramic (Al₂O₃) particles. *Materials & Design*, 59, 246-251.
- Lee, K. B., Sim, H. S., Heo, S. W., Cho, S. Y., & Kwon, H. (2000). Fabrication of Al alloys reinforced with AlN particles formed by in-situ reaction. *Metals and Materials*, 6(1), 25-32.
- Lee, K. S., Jo, Y. M., & Lee, Y. S. (2013). Crystallization and high-temperature deformation behavior of Cu₄₉Zr₄₅Al₆ bulk metallic glass within supercooled liquid region. *Journal of Non-Crystalline Solids*, 376, 145-151.
- Louzguine-Luzgin, D. V., Xie, G. Q., Gonzales, S., Wang, J. Q., Nakayama, K., Perepezko, J. H., & Inoue, A. (2012). Nano-crystallization behavior of Zr–Cu–Al bulk glass-forming alloy. *Journal of Non-Crystalline Solids*, 358(2), 145-149.
- Lv, L., Lai, M. O., Su, Y., Teo, H. L., & Feng, C. F. (2001). In situ TiB₂ reinforced Al alloy composites. *Scripta Materialia*, 45(9), 1017-1023.
- Mazahery, A., Abdizadeh, H., & Baharvandi, H. R. (2009). Development of high-performance A356/nano- Al₂O₃ composites. *Materials Science and Engineering: A*, 518(1), 6164.
- Pauly, S., Das, J., Mattern, N., Kim, D. H., & Eckert, J. (2009). Phase formation and thermal stability in Cu–Zr–Ti (Al) metallic glasses. *Intermetallics*, 17(6), 453-462.
- Qin, S., Chen, C., Zhang, G., Wang, W., & Wang, Z. (1999). The effect of particle shape on ductility of SiCp reinforced 6061 Al matrix composites. *Materials Science and Engineering: A*, 272(2), 363-370.
- Roy, D., Basu, B., & Mallick, A. B. (2005). Tribological properties of Ti-aluminide reinforced Al-based in situ metal matrix composite. *Intermetallics*, 13(7), 733-740.
- Roy, D., Basu, B., Mallick, A. B., Kumar, B. M., & Ghosh, S. (2006). Understanding the unlubricated friction and wear behavior of Fe-aluminide reinforced Al-based in-situ metal–matrix composite. *Composites Part A: Applied Science and Manufacturing*, 37(9), 1464-1472.
- Roy, D., Ghosh, S., Basumallick, A., & Basu, B. (2007). Preparation of Ti-aluminide reinforced in situ aluminium matrix composites by reactive hot pressing. *Journal of alloys and compounds*, 436(1), 107-111.
- Sharifi, E. M., & Karimzadeh, F. (2011). Wear behavior of aluminum matrix hybrid nanocomposites fabricated by powder metallurgy. *Wear*, 271(7), 1072-1079.
- Wielage, B., Zschunke, M., Henker, A., & Steinhäuser, S. (1996). Manufacture and characterization of particle reinforced aluminum coatings. In C. C. Berndt (Ed.), *Thermal Spray: Practical Solutions for Engineering Problems* (pp. 333-337). Ohio: ASM International.
- Wu, Y., Wang, H., Wu, H. H., Zhang, Z. Y., Hui, X. D., Chen, G. L., ... & Lu, Z. P. (2011). Formation of Cu–Zr–Al bulk metallic glass composites with improved tensile properties. *Acta Materialia*, 59(8), 2928-2936.

- Xie, G., Louzguine-Luzgin, D. V., Fukuhara, M., Kimura, H., & Inoue, A. (2010). Cu particulate dispersed $\text{Cu}_{50}\text{Zr}_{45}\text{Al}_5$ bulk metallic glassy composite with enhanced electrical conductivity. *Intermetallics*, 18(10), 1973-1977.
- Yamasaki, T., Zheng, Y. J., Ogino, Y., Terasawa, M., Mitamura, T., & Fukami, T. (2003). Formation of metal-TiN/TiC nanocomposite powders by mechanical alloying and their consolidation. *Materials Science and Engineering: A*, 350(1), 168-172.
- Zhang, L. K., Chen, Z. H., Zheng, Q., & Chen, D. (2013). Isochronal and isothermal phase transformation of $\text{Cu}_{45}\text{Zr}_{45}\text{Ag}_7\text{Al}_3$ bulk metallic glass. *Physica B: Condensed Matter*, 411, 149-153.

Copyrights

Copyright for this article is retained by the author(s), with first publication rights granted to the journal.

This is an open-access article distributed under the terms and conditions of the Creative Commons Attribution license (<http://creativecommons.org/licenses/by/3.0/>).